

Optical spectral signatures of dusty starburst galaxies

Bianca M. Poggianti^{1,2,3} & Hong Wu^{4,2}

1) Osservatorio Astronomico di Padova, vicolo dell'Osservatorio 5, 35122 Padova, Italy

2) Institute of Astronomy, Madingley Rd, Cambridge CB3 0HA, UK

3) Royal Greenwich Observatory, Madingley Rd, Cambridge CB3 0EZ, UK

4) Beijing Astronomical Observatory, Chinese Academy of Sciences, Beijing 100080, China

ABSTRACT

We analyse the optical spectral properties of the complete sample of Very Luminous Infrared Galaxies presented by Wu et al. (1998a,b) and we find a high fraction ($\sim 50\%$) of spectra showing both a strong $H\delta$ line in absorption and relatively modest $[OII]$ emission (e(a) spectra). The e(a) signature has been proposed as an efficient method to identify dusty starburst galaxies and we study the star formation activity and the nature of these galaxies, as well as the effects of dust on their observed properties. We examine their emission line characteristics, in particular their $[OII]/H\alpha$ ratio, and we find this to be greatly affected by reddening. A search for AGN spectral signatures reveals that the e(a)'s are typically HII/LINER galaxies. We compare the star formation rates derived from the FIR luminosities with the estimates based on the $H\alpha$ line and find that the values obtained from the optical emission lines are a factor of 10-70 ($H\alpha$) and 20-140 ($[OII]$) lower than the FIR estimates ($50-300 M_{\odot} yr^{-1}$). We then study the morphological properties of the e(a) galaxies, looking for a near companion or signs of a merger/interaction. In order to explore the evolution of the e(a) population, we present an overview of the available observations of e(a)'s in different environments both at low and high redshift. Finally, we discuss the role of dust in determining the e(a) spectral properties and we propose a scenario of selective obscuration in which the extinction decreases with the stellar age.

Subject headings: galaxies: clusters: general — galaxies: evolution — infrared: galaxies

Received _____; accepted _____

1. Introduction

The remarkable achievements of a number of recent optical observations of distant galaxies have delineated a picture of the star formation history of the Universe at redshift $0 < z < 5$ (see reviews from Ellis 1998a, 1998b and references therein; Steidel et al. 1999). At the same time, this progress has accentuated the necessity of evaluating the role played by dust in obscuring star-forming systems (Meurer et al. 1997, Pettini et al. 1998, Dickinson 1998, Steidel et al. 1998, Glazebrook et al. 1999) and has strongly reminded the astronomical community that relying on optical data alone is likely to offer a partial view of the evolutionary history of galaxies, certainly quantitatively incomplete and possibly qualitatively incorrect.

A major remained challenge is thus to assess the amount of star formation activity hidden by dust in the objects detected and uncover eventual entire galactic populations which might have been missed by the optical census. Deep surveys in the submillimeter regime with SCUBA (Smail et al. 1997, 1998a, Hughes et al. 1998, Barger et al. 1998, Lilly et al. 1999, see Smail et al. 1998b for a review) and in the Mid/Far-Infrared with ISO (Flores et al. 1998a,b, Elbaz et al. 1998, Altieri et al. 1999, Aussel et al. 1999, Puget et al. 1999, Clements et al. 1999, Metcalfe et al. 1999, Oliver et al. 1999) are starting to unveil high/intermediate redshift populations of galaxies whose star formation is hidden/underestimated at optical wavelengths. A full exploitation of this observational break-through at long wavelengths relies on the comparison with optical and near-infrared data for the identification of the counterparts of these sources, for the determination of their redshift and for investigating the nature of the source of the submillimeter/IR emission.

A key question is whether the distant, dusty star-forming galaxies are recognizable from optical/near-IR data alone. Heavily reddened sources cannot be unambiguously identified by optical and near-IR colors: photometry of even the most extreme cases ($R - K > 5 - 6$, EROs, Extremely Red Objects) cannot establish whether these objects are heavily reddened starbursts at high- z (Graham & Dey 1996, Cimatti et al. 1998, Dey et al. 1999) or high redshift analogs of local elliptical galaxies (Spinrad et al. 1997, Cohen et al. 1999, Treu et al. 1999). Thus finding an optical *spectroscopic* signature able to pick out highly extincted galaxies would be extremely valuable, especially given the large number of spectra accessible from recent and near-future spectroscopic surveys.

First evidence for the existence of such a signature has emerged from distant cluster studies. Dressler et al. (1999, D99) presented a spectroscopic catalog of cluster and field galaxies at $z \sim 0.4 - 0.5$ and identified a class of spectra with strong Balmer lines in absorption and [OII] in emission (hereafter “e(a)” galaxies, $\text{EW}(\text{H}\delta) > 4 \text{ \AA}$ and $\text{EW}(\text{OII}) > 5 \text{ \AA}$), which was found to be abundant at intermediate redshifts both in the cluster and in the field environment (about 10 % of the entire galactic population in D99, see also Poggianti et al. 1999, P99). These authors also found a numerous *cluster* population of galaxies with strong Balmer lines in absorption and no detectable emission-lines (“k+a/a+k” class, $\text{EW}(\text{H}\delta)_0 > 3 \text{ \AA}$, traditionally named “E+A” galaxies), which are universally interpreted as post-starburst/post-starforming galaxies in which the star formation ended between a few Myr and 1.5 Gyr before the time of observation (P99).

On the basis of dust-free models, the e(a) spectra appear associated with *post-starburst* galaxies with some residual star formation (P99). However, a search for similar spectra in the local Universe (P99) revealed that they are frequent among merging/strongly interacting galaxies (40 % in the sample of Liu & Kennicutt 1995a,b, LK95a,b), while they are scarce in normal field galaxy samples (8–7 % in the Las Campanas Redshift Survey and in Kennicutt 1992a,b, K92a,b, see §5.1 for details). All of the e(a) galaxies

in LK95 are strong FIR emitters and are known to be highly extinguished starbursts.

From the comparison of the distant e(a) galaxies with their low- z counterparts and the similarity of their spectral properties (in particular, their low $\text{EW}(\text{OII})/\text{EW}(\text{H}\alpha)$ ratios), P99 concluded that the e(a) galaxies are starbursts which contain a substantial amount of dust and suggested that they might be the progenitors of the abundant cluster population of post-starburst galaxies (k+a/a+k). They also tentatively explained the e(a) peculiar spectral properties as the result of “selective” dust extinction, which affects the youngest, most massive stars in HII regions much more than the older stellar populations responsible for the continuum flux.

It is clear that if the e(a) signature is proved to be unequivocally associated with highly extinguished starbursts, then the identification of a strong H δ line in emission-line spectra is a very powerful method to detect dusty-starforming galaxies up to high redshift. Since in this case the SFR estimates based on optical data are unreliable, it is important to establish whether the detection of e(a) spectra, besides revealing the *presence* and *incidence* of a starburst population, also allows to *quantify* the amount of star formation hidden by the dust and whether it provides definite informations about the properties and nature of these galaxies. These final issues could not be investigated on the basis of the D99 distant cluster sample, for which independent means of deriving the SFRs (e.g. FIR data) are not available. Hence a number of questions have remained open:

- a) Are *all* the e(a) spectra associated with dusty starbursts? i.e. What is the range of FIR luminosities of the e(a) galaxies?
- b) What fraction of the dusty starburst population display en e(a) spectrum? i.e. What is the proportion of e(a) galaxies as a function of the FIR luminosity?
- c) What are their typical star formation rates? What percentage is hidden by dust?
- d) Which star formation and dust properties/geometries are responsible for the e(a) spectral characteristics?
- e) Are e(a) spectra always connected with merging galaxies, or are there other mechanisms that can produce them?
- f) What is the frequency of e(a) galaxies as a function of redshift and environment?

The goal of this paper is to investigate some of these issues by analysing the sample of Very Luminous Infrared Galaxies (VLIRGs, $\log(L_{\text{IR}}/L_{\odot}) \geq 11.5$) presented in Wu et al. (1998a,b W98a,b). This sample has a number of advantages for the purpose of our study: it is the largest, complete sample of VLIRGs obtained to date, comprising a number of objects adequate for a statistical study. The wealth of information available for these galaxies (emission-line luminosities over a wide spectral range, FIR luminosities, merger stage/morphologies, reddening estimates) makes it an excellent dataset for testing the connection between e(a) spectra and dusty starbursts and for inspecting the properties of galaxies characterized by this type of spectra. The ultimate purpose of this analysis is to investigate the nature of the e(a) galaxies in general and hopefully shed some light on the properties of the distant e(a)’s found in deep spectroscopic surveys.

The plan of the paper is as follows: in the next section we briefly present the spectroscopic catalog and we describe the line measurements and the spectral classification (§2.1). In §3 we show the results of our spectral analysis and we examine the distributions of “activity” (AGN) type of our spectral classes. In §4 we compare the spectral characteristics with other galactic properties (FIR luminosities, reddening estimates,

morphologies) in order to establish the typical dust obscuration, star formation rates and merger stage of the e(a) population. In §5 we review the incidence of e(a)’s in other spectroscopic surveys both at low and high redshift and in §6 we examine the possible physical scenarios accounting for the observed spectral properties (§6.1). We then summarize our main conclusions in §7. We assume $H_0 = 50 \text{ km s}^{-1} \text{ Mpc}^{-1}$ and $q_0 = 0.5$.

2. The spectroscopic catalog

In this paper we will make use of the spectroscopic catalog of very luminous infrared galaxies obtained by W98a,b. W98a observed a complete sample (73 galaxies, hereafter the “VLIRG sample”) selected from the 2 Jy redshift survey (Strauss et al. 1992) with $\log(L_{IR}/L_\odot) \geq 11.5$ and sufficiently optically bright to obtain good S/N spectra. The 2 Jy survey includes all the objects from the IRAS Point Source catalog with $f_{60} > 1.936 \text{ Jy}$, $f_{60}^2 > f_{12}f_{25}$ (a color criterion distinguishing galaxies from Galactic objects) and Galactic latitude $|b| > 5^\circ$.

In addition, spectra for 40 companions of VLIRG galaxies and for 10 galaxies with slightly lower FIR luminosity/fainter optical magnitudes were obtained (W98a). In the following we will refer to the 40 companion galaxies as the “companion sample” and to the total sample (VLIRG+companion) as the “total W98 sample”. Most of these sources lie in the redshift range $0.02 < z < 0.05$ and have $\log(L_{IR}/L_\odot)$ between 11.5 and 12 (see W98a for the redshift and infrared luminosity distributions). For the purposes of this paper we have included into the VLIRG sample 9 of the additional 10 galaxies with fainter/unknown optical magnitudes (6 objects) or $\log(L_{IR}/L_\odot) \geq 11.465$ (3 objects), excluding only 1 galaxy significantly fainter in the FIR (09517+6954, $\log(L_{IR}/L_\odot) = 10.833$). Three companion and one VLIRG spectra are too poor to determine their redshift/spectral class and have been disregarded in the analysis.

The spectra were obtained with the 2.16 m telescope at the Beijing Astronomical Observatory and cover the spectral range either 4400–7100 Å or 3500–8100 Å at a resolution of 11.2 and 9.3 Å respectively.¹ The apertures were varied according to the redshift and correspond to the central 2 kpc for galaxies with $z < 0.034$, while for the most distant objects (about 40 % of the sample) a larger area is covered.

In addition to the FIR luminosities², W98a,b list the relative fluxes of a number of emission–lines, the observed H α fluxes, the equivalent widths (EWs) of H α and the intrinsic reddening estimates. We stress that, since many galaxies in the W98 sample are in pairs, multi–nuclei systems or groups, in some cases the task of identifying the component emitting the FIR luminosity is problematic. For most galaxies the identification was done using the IRAS position and error ellipse, while for those sources with more than one companion in the error ellipse, the optical counterpart was found from the infrared colors or order of activity (Seyfert1, Seyfert2, LINER, HII) (W98b). For four of the sources (08507+3520, 13373+0105,

¹A full description of the data reduction procedure and of the spectra obtained can be found in W98a.

²The FIR luminosities given from W98a are computed from the 60 μm and 100 μm fluxes ($F_{IR} = 1.75[2.55S_{60} + 1.01S_{100}]10^{-14} \text{ W m}^{-2}$). These are approximately total FIR luminosities in the range 1–1000 μm . Following the definition of “total far–infrared emission” given by Helou et al.(1988) and adopting a standard correction factor 1.5 to convert the 42.5–122.5 μm emission into a 1–1000 μm flux, the factors (1.75;2.55;1.01) in the formula above would be replaced by (1.89;2.58;1.00).

13458+1540, 13496+0221) it was impossible to determine which companion accounts for the FIR emission and this has been assigned to each one of the components. For at least some of the sources, the FIR emission probably comes from two or even more companions, hence the discrimination between a VLIRG and a companion galaxy can be somewhat arbitrary and the companion sample should not be regarded in any way as a “low-FIR luminosity” sample.

2.1. Spectral measurements and classification

In order to study the star formation and dust properties of these galaxies it is useful to classify their spectra into a number of classes. We adopt here a spectral classification scheme similar to the one presented in D99. This scheme (Table 1) is based on two lines, $[\text{OII}]\lambda 3727$ in emission and $\text{H}\delta(\lambda = 4101 \text{ \AA})$ in absorption, which are good indicators of (respectively) current and recent star formation in distant galaxy spectra.

We measured the strength of these two lines and of the other main spectral features with two methods: using the package SPLOT within the IRAF environment (comparing the results found with a Gaussian fit and interactively choosing the line endpoints) and using the same purpose-written software as in D99. The two methods gave consistent results, and in the case of the $\text{H}\alpha + \text{NII}$ blend our measurements are in good agreement with the values listed in W98a,b. Since we wish to compare our results with those obtained by D99, in the following we will use the values derived with their method. Repeated measurements show that the typical uncertainty in the EWs is $\sim 20\%$ for the weakest lines and a few per cent for the strongest ones.

Examples of the main emission-line classes classified according to the $\text{H}\delta$ and $[\text{OII}]$ strength are shown in Fig. 1. The $\text{H}\delta$ line is prominent in absorption in the e(a) spectrum (top panel, 6 \AA), while it is absent/weak in emission in the other two spectra.

TABLE 1
SPECTRAL CLASSIFICATION SCHEME

Class	EW($[\text{OII}] 3727$) (\AA)	EW($\text{H}\delta$) (\AA)	Comments
k	absent	< 3	passive
k+a/a+k	absent	≥ 3	strong Balmer absorption without emission
e(c)	yes, < 40	< 4	moderate Balmer absorption plus emission, spiral-like
e(a)	yes	≥ 4	strong Balmer absorption plus emission
e(b)	≥ 40	any	very strong $[\text{OII}]$
sey1	any	any	Seyfert1 from broad hydrogen lines in emission
e	yes	?	at least one emission line, $\text{H}\delta$ unmeasurable

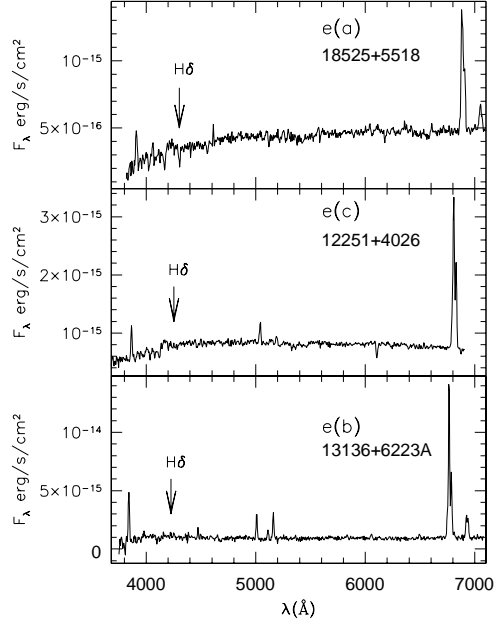


Fig. 1. Representative spectra of the e(a), e(c) and e(b) classes. A limited spectral range including both the [OII] and the H α lines is displayed. The position of the H δ line is shown in each panel with an arrow. The complete spectroscopic catalog is presented in W98a.

A detailed modeling of each spectral class can be found in P99. Here we briefly summarize their conclusions and proposed interpretation of each class:

k type: passive, elliptical-like spectrum of a galaxy with neither on-going nor recent star formation.

k+a/a+k type: spectrum of a post-starburst/post-starforming galaxy with no current star formation which was forming stars at a vigorous rate in the recent past (last 1.5 Gyr).

e(c) type: typical spectrum of a spiral at low redshift which has been forming stars in a continuous fashion (without bursts) for the last 2 Gyr or longer.

e(a) type: spectrum of a dust-enshrouded starburst galaxy.

e(b) type: spectrum with very strong emission lines of a galaxy which is undergoing strong star formation.

sey1 type: Seyfert1 spectrum with broad emission lines.

e type: spectrum of a galaxy with current star formation. Since the H δ line is unmeasurable (in most cases because it falls out of the observed spectral range) we cannot classify it into one of the emission line classes described above.

3. Results

TABLE 2
VLIRG GALAXIES

IRAS name	spec. class	L_{IR}/L_{\odot}^a (log)	AGN type ^b	EW [OII] (Å)	EW(H β) (Å)	EW(H α + NII) (Å)	EW(H δ) (Å)	EW [OIII] ^c (Å)	SFR _{FIR} ^d M_{\odot}/yr	SFR _{Hα} ^d M_{\odot}/yr
(1)	(2)	(3)	(4)	(5)	(6)	(7)	(8)	(9)	(10)	(11)
00189+3748A	e(a)	11.572	LH	14.3	7.2	86.5	4.6	1.4	64.2	2.17
00267+3016A	e(a)	11.966	L	10.9	2.4	75.6	4.1	4.1	159.0	5.51
00509+1225	sey1	11.772	S1	3.1	19.9	143.4	-2.6	14.6	101.7	42.89
01173+1405	e(b)	11.868	LH	42.5	11.8	145.6	0.0	10.6	126.9	1.12
01324+2138	e(a)	11.629	LH	25.8	4.7	75.8	7.9	15.6:	73.2	2.27
01484+2220	e	11.851	H	out	5.3	59.0	out	1.2	122.0	1.61
01572+0009	sey1	12.665	S1	2.5	20.2	177.3	fil	32.3	795.3	163.36
02071+3857	e(a)	11.546	H	out	fil	34.1	13.3	0.8	60.5	1.08
02203+3158A	e(a)	11.837	LH	6.2	2.4	46.2	6.5	4.5	118.2	1.94
02222+2159	e	11.652	H	?	0.0	35.3	0.0	2.1	77.2	0.98
02248+2621	e(c)	11.519	H	9.0	9.5	160.7	?	5.0	56.8	6.94
02435+1253	e(a)	11.501	LH	25.6:	0.0	43.4	9.7	5.1	54.5	0.24
02512+1446A	e	11.780	H	12.6	10.9	141.2	?	5.3:	103.6	1.73
03117+4151A	e(b)	11.562	S2	66.7	17.4	207.1	0.0	93.8	62.7	5.25
05084+7936	e(a)	12.170	H	35.6	8.0	101.8	7.8	?	254.4	6.62
05414+5840	e	11.505	S?	out	-7.7	17.7	0.0	?	55.0	0.06
06538+4628	e	11.490	H	out	12.0	128.2	?	6.2	53.2	4.61
07062+2041B	e(a)	11.559	H	18.2	5.9	64.5	4.9	4.1	62.3	1.47
07063+2043A	e(a):	11.570	H	out	4.3	70.1	8.2:	2.5	63.9	1.55
07256+3355A	e(a)	11.467	H	6.9	3.4	66.6	5.3	1.2:	50.4	1.14
08354+2555	e(a) ⁺	11.781	S?	0.0	-5.3	23.0	7.2	—	103.9	0.32
08507+3520A	e(c)	11.811	S?	0.0	4.3	22.8	0.0	3.1:	111.3	1.03
08507+3520B	e(b,a):	11.811	S?	73.0	5.5	44.7	9.2:	9.7:	111.3	1.31
08507+3520C	e	11.811	S?	< 19.1	7.7	55.9	?	10.1	111.3	1.00
09047+1838	e(a)	11.490	H	11.6	4.7	59.7	4.2	1.5	53.2	1.22
09126+4432A	e(a):	11.913	LH	10.3	0.0	29.2	1.5:	1.5	140.8	1.03
09168+3308	e(a):	11.725	H	18.0	8.8	84.2	?	4.0	91.3	3.41
09320+6134	e(a)	12.220	L	18.9	fil	63.5	8.6	4.6	285.4	1.79
09333+4841A	e(a)	11.523	H	16.1	3.0	60.9	5.7	3.6	57.3	1.26
10203+5235	e(c)	11.620	L	25.6	5.9	71.7	3.6	8.2	71.7	1.94
10311+3507	e	12.096	H	out	13.5	113.5	out	2.7	214.5	15.25
11231+1456A	e(c)	11.809	LH	14.3	5.9	84.9	2.3	1.1:	110.8	1.90
11254+1126	e	11.800	LH	out	5.3	89.9	out	8.6	108.5	4.48
11257+5850B	e	12.040	LH	out	30.6	219.5	out	29.7	188.6	0.67
11543+0124	e(a)	11.716	LH	13.8:	0.0	40.5	6.1	2.0	89.4	1.50
12112+0305A	e(c)	12.531	LH	35.2	5.3	88.2	fil	13.3	584.2	3.21
12120+6838A	e	12.029	LH	out	4.3	53.6	out	4.1	183.9	2.33
12251+4026	e(c)	11.660	H	13.3	6.5	91.5	fil/emi	3.7	78.6	2.96
12265+0219	sey1	12.663	S1	0.0	40.3	203.8	emi	6.3:	791.6	2316.27
12323+1549B	e(c)	11.766	S1	6.7	15.9	104.9	0.0	8.8	100.4	8.23
12540+5708	sey1	12.635	S1	out	?	122.8	out	6.2:	742.2	188.40
12592+0436	e(a)	11.787	L	4.6	-6.9	28.8	4.4	?	105.3	0.40
13136+6223A	e(b)	11.937	H	102.2	34.8	203.5	emi	27.8:	148.8	8.86
13183+3423	e	11.863	LH	out	1.0	88.3	out	4.5	125.5	0.97
13299+1121	e	11.516	H	out	28.6	235.0	out	17.1	56.4	9.14
13362+4831B	e	11.706	S2	out	15.2	160.7	out	87.7	87.4	2.05
13373+0105A	e	11.701	LH	out	?	17.9	out	—	86.4	0.22
13373+0105B	e	11.701	H	out	19.4	144.3	out	14.4	86.4	1.36
13428+5608	e	12.392	S2	out	9.9	205.4	out	60.2	424.2	5.95
13458+1540A	e(a)	11.821	H	13.3	5.8	98.4	4.9	2.9	113.9	5.02
13458+1540B	e(c)	11.821	H	13.7	4.9	68.6	fil	4.7	113.9	2.53
13496+0221A	e(a)	11.752	H	8.9	0.0	24.2	4.5	—	97.2	0.70
13496+0221B	e	11.752	H	25.5	3.2	30.3	4.6:	—	97.2	0.92
13536+1836	e	11.611	S2	out	37.5	457.3	out	312.2	70.2	25.89

TABLE 2 – CONTINUED
VLIRG GALAXIES

IRAS name	spec. class	L_{IR}/L_{\odot}^a (log)	AGN type ^b	EW [OII] (Å)	EW(H β) (Å)	EW(H α + NII) (Å)	EW(H δ) (Å)	EW [OIII] ^c (Å)	SFR _{FIR} ^d M_{\odot}/yr	SFR _{Hα} ^d M_{\odot}/yr
(1)	(2)	(3)	(4)	(5)	(6)	(7)	(8)	(9)	(10)	(11)
14151+2705A	e(a)	11.565	LH	3.4:	< -7.7	24.3	5.4	1.0:	63.2	2.04
14178+4927	e(a):	11.541	LH	0.0	4.3	72.2	3.9	1.4	59.8	1.10
14547+2448A	e	11.897	L	out	2.5	36.8	out	6.2	135.7	0.57
14568+4504	e	11.501	LH	out	4.4	57.7	out	8.1	54.5	2.79
15107+0724	e(c)	11.525	H	out	0.0	30.7	?	—	57.6	0.08
15163+4255	e	12.072	H	out	17.4	235.4	out	15.2	203.0	8.27
15327+2340	e	12.464	S?	out	?	44.1	out	13.3:	500.6	0.06
15425+4114A	e	11.515	H	out	5.8	79.9	out	7.3	56.3	2.28
15426+4116B	e	11.546	LH	out	3.2	10.4	out	—	60.5	0.53
16104+5235	e	11.687	H	out	34.7	328.0	out	14.4	83.7	12.90
16180+3753	e	11.592	H	out	7.4	44.4	out	?	67.2	1.74
16284+0411	e	11.582	LH	out	5.0	87.2	out	—	65.7	1.13
16504+0228	e	12.028	L	out	17.5	269.3	out	19.4	183.5	1.55
16577+5900A	e	11.582	LH	out	3.9	31.1	out	—	65.7	0.26
16589+0521	e(c)	11.637	H	21.3	7.7	89.7	0.0	3.6	74.6	2.99
17366+8646	e(a):	11.544	H	10.2	1.7	56.9	4.0	2.0	60.2	1.08
17392+3845	e	11.554	H	out	4.8	48.7	out	?	61.6	2.98
17501+6825A	e	11.829	H	out	8.9	82.3	out	5.2	116.0	4.64
18525+5518	e(a)	11.683	H	19.0	3.3	53.5	6.0	4.3:	82.9	2.16
18595+5048	e(c)	11.501	LH	17.2	1.6	44.2	0.0	1.9	54.5	0.77
19120+7320A	e	11.624	S2	12.1	4.7	87.9	2.0:	21.5	72.4	1.33
20550+1656	e(b)	12.074	H	75.6	38.7	305.2	-5.4	83.4	204.0	19.44
22388+3359	e(c):	11.531	LH	7.5	fil	39.4	3.4:	—	58.4	0.41
22501+2427	e(c)	11.723	H	1.5	10.7	162.1	fil	4.2	90.9	6.73
23007+0836A	sey1	11.734	S1	3.0	22.4	174.6	emi	27.1	93.2	10.03
23024+1916	e	11.573	LH	out	5.2	64.8	out	5.6	64.3	0.64
23135+2516	e(a)	11.730	LH	16.2	2.0	52.3	4.1	8.6	92.4	1.11
23254+0830A	e	11.568	H	7.0	?	35.0	?	—	63.6	2.55
23488+1949A	e	11.528	H	4.5	4.0	60.4	1.5:	1.1	58.0	1.56
23488+2018A	e(a)	11.609	H	11.9	5.6	93.1	4.1	2.7:	69.9	1.71
23532+2513A	e(a):	11.795	H	?	abs	31.5	5.5:	?	107.3	1.12
23594+3622	e(a):	11.586	S2	26.5	abs	62.5	2.5:	4.4	66.3	0.69

^a From W98a.

^b From W98b, see §3.1.

^c [OIII] λ 5007.

^d SFR estimated from the FIR and H α luminosity, see §4.2.

EWs are given in the rest frame.

A colon mark “:” indicates an uncertain value or class.

“e(a)+” = H α emission, no detectable [OII] and strong H δ absorption.

“out” = line unmeasurable because out of the spectrum range.

“fil” = line filled by the emission component.

“emi” = line in emission but unmeasurable.

“?” = line unmeasurable.

TABLE 3
COMPANION GALAXIES

IRAS name	spec. class	AGN type ^b	EW [OII] (Å)	EW(H β) (Å)	EW(H α + NII) (Å)	EW(H δ) (Å)	EW [OIII] ^c (Å)
(1)	(2)	(3)	(4)	(5)	(6)	(7)	(8)
00189+3748B	e(a):	LH	15.2	3.1	46.2	11.2	2.2
00267+3016B	e(a)	LH	8.9	3.0	74.4	> 7.3	5.5:
02203+3158B	e(a)	H	5.1	2.3	38.4	4.6	—
07256+3355B	e(c)	H	0.0	4.3	34.9	2.3	—
07256+3355C	k	O	0.0	0.0	0.0	0.0	—
09126+4432B	e(a):	H	?	emi	40.8	9.8	?
09333+4841B	e	H	32.5:	2.4	26.2	?	5.7:
11231+1456B	e(c)	LH	5.8	4.1	50.4	0.0	1.5:
11257+5850A	e	H	out	36.6	217.4	out	30.7
12112+0305C	e(c)	LH	24.2	6.8	76.1	0.0	15.5
12120+6838C	e(a): ⁺	LH	0.0	0.0	12.3	4.1:	—
12120+6838D	e	H	21.3	5.9	49.3	?	4.1
12323+1549A	e(c)	LH	?	0.0	9.6	1.6	—
13136+6223B	e	LH	?	?	57.4	?	8.9:
13362+4831A	e	L	out	24.9	225.4	out	41.3
13496+0221C	e	H	24.8	7.9	30.5	?	—
14151+2705B	e(a):	H	21.6:	0.0	5.1:	9.0:	—
14547+2448B	e(a):	H	19.1:	8.0	49.7	5.3:	—
16577+5900B	e	LH	out	2.1	35.0	out	3.3
17501+6825B	e(c)	LH	26.7	5.8	71.4	fil	14.0
17501+6825C	e(a)	H	14.6:	2.6:	32.3	5.4	3.0:
17501+6825D	e(c)	LH	11.1	4.9	43.2	3.0:	1.4:
19120+7320B	e(c)	H	13.5	10.2	95.5	fil	1.4:
23007+0836B	e(c)	S?	0.0	fil	40.8	0.0	?
23254+0830B	e(b)	S2	45.6	25.4	263.0	fil	248.7:
23254+0830C	e	O	5.3	?	0.0	?	?
23254+0830D	k	O	0.0	-2.8	0.0	1.2	?
23488+1949B	e(c)	H	33.9	15.8	146.4	0.0	13.1
23488+1949C	e(a): ⁺	LH	0.0	3.9	61.6	?	—
23488+2018B	e	H	out	9.1	35.9	out	15.6
23532+2513B	sey1	S1	0.0	31.4	120.8	emi	8.6
23532+2513C	e(a):	H	12.1	4.3	59.5	8.1:	6.1

Notes as in Table 2.

IR07256+3355C, IR12323+1549A and IR23254+0830C should be unrelated to the FIR source (background/foreground galaxies).

In this section we present the results of our spectral analysis and we assess the incidence of each spectral class among Very Luminous Infrared Galaxies. By comparing the strength and the correlations between the various spectral features with those observed in optically selected samples, we aim at studying the stellar and dust properties of these galaxies and the eventual presence of an AGN component in their spectra.

The spectral classification and our measurements of the rest frame equivalent widths are shown in Table 2 (VLIRG sample) and Table 3 (companion sample). Lines seen in emission are given a positive equivalent width, with the exception of the $H\delta$ line which is given a positive value when it is observed in absorption.

In Table 4 we list the proportion of galaxies as a function of the spectral class; they are normalized to the total number of spectra with a *securely assigned spectral type*, excluding the “e” spectra that are 40% and 28% of the VLIRG and companion sample respectively. The errors quoted are found assuming Poissonian statistics.

Table 4 shows that all the VLIRGs and the great majority of the companion galaxies have emission lines and this confirms that – at least qualitatively – the FIR and the optical data agree on revealing the existence of on-going star formation activity. Among the VLIRGs the incidence of e(a) spectra ³ is very high (56 %). About 1/4 of the VLIRGs have an e(c) “spiral-like” spectrum, while only 1 out of 10 have very strong [OII] emission (e(b) class). Broad hydrogen lines denoting Seyfert1 spectra are observed in 10 % of the VLIRGs.

Similar spectral fractions are found among the companion galaxies but with a slightly lower e(a) proportion (43 %), an additional passive component (k class, 9 %) and a higher proportion of normal “spiral-like” spectra (e(c) class, 39 %). Notably no k+a/a+k spectrum is found in the whole W98 catalog; we will comment this result later in §6. It is interesting that there is a strong tendency for e(a) galaxies to have e(a) companions: from Table 2 we find 6 e(a)–e(a) associations, 3 e(c)–e(c) companions and only 1 “mixed couple” e(a)–e(c).

The equivalent widths of [OII] and $H\delta$ of the W98 galaxies are plotted in the top panel of Fig. 2, where the e(c), e(b) and k spectra have been grouped into the “non-e(a)” class. The EWs of the merging galaxies (LK95) (Fig. 2, lower panel) are similar to those of the Infrared Luminous galaxies, but the merger sample

³Three galaxies with a strong $H\delta$ line in absorption and no detectable [OII] line have been included into the e(a) class because they display a clear $H\alpha$ line in emission (e(a)⁺). We note that at higher redshift ($z \geq 0.4$) these spectra would be classified as k+a galaxies because the $H\alpha$ line is redshifted out of the optical range; hence the “true” e(a) fraction in distant surveys could be higher than it is observed (P99).

TABLE 4
FRACTION OF GALAXIES AS A FUNCTION OF THE SPECTRAL CLASS

Class	VLIRG	N_{VLIRG}	companion.	$N_{companion.}$	total
e(a)	0.56 ± 0.10	29	0.43 ± 0.14	10	0.52 ± 0.08
e(c)	0.25 ± 0.07	13	0.39 ± 0.13	9	0.29 ± 0.06
e(b)	0.10 ± 0.04	5	0.04 ± 0.04	1	0.08 ± 0.03
sey1	0.10 ± 0.04	5	0.04 ± 0.04	1	0.08 ± 0.03
k	0	0	0.09 ± 0.06	2	0.03 ± 0.02

has a greater proportion of non- $e(a)$ galaxies. The normal galaxies (K92a) occupy a confined region of the diagram with $EW(H\delta) < 4 \text{ \AA}$ and $EW([OII]) < 20 \text{ \AA}$. The $EW([OII])$ s of $e(a)$ and “normal” galaxies tend to increase with $EW(H\delta)$ (Fig. 2) and this suggests that the production and/or visibility of the nebular emission is related to the abundance and/or visibility of the stellar populations responsible for the strong $H\delta$.

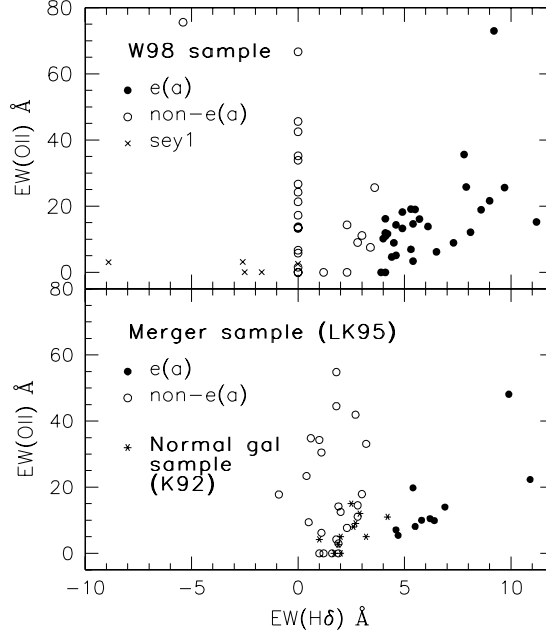


Fig. 2. $EW([OII])$ versus $EW(H\delta)$ for the total W98 sample (top panel), the merging galaxies sample from LK95 (bottom panel; whole aperture/integrated (when available) or nuclear spectra) and the normal galaxies from K92 (types E to Sc with no sign of a starburst or interaction/merger, bottom panel; spectra are integrated). The non- $e(a)$ spectra ($e(c)$, $e(b)$, k) are represented by the empty dots. Since the program that computes the line strength is not suitable to measure weak or undetectable lines, in the top panel a value =0 have been assigned to the weakest $H\delta$ equivalent widths, which in any case are smaller than 2 \AA . Note that most of the Seyfert1 spectra (crosses in the top panel) display the $H\delta$ line in emission and have a very weak $[OII]$ line.

A notable property of the $e(a)$ galaxies appears to be a low $EW(OII)/EW(H\alpha+NII)$ ratio; this has been observed in the $e(a)$ spectra of distant cluster galaxies and of nearby mergers (P99). We find the same characteristic also in the galaxies of the W98 sample: in the EW-EW diagram (Fig. 3) the great majority of points lie on the right side of the straight line, which represents a rough fit for normal field galaxies at low-redshift. The median $EW([OII])/EW(H\alpha+NII)$ ratios of the VLIRG and the total W98 sample are 0.21 ± 0.04 and 0.20 ± 0.03 respectively. These are a factor of 2 lower than the ratio found for optically-selected nearby galaxies ($0.42-0.47$, K92, Tresse et al. 1999). In the scenario proposed by P99, these low EW ratios are due to high dust extinction: the HII regions where the line emission is produced are deeply embedded in large amounts of dust, which affects the $[OII]$ line more than $H\alpha$. Since the continuum underlying the lines is produced by older, less extincted stars, the net result is a low EW ratio of the two lines. It is remarkable that in the Infrared Luminous sample *both the $e(a)$ and the non- $e(a)$ spectra have low ratios*, while in the optically-selected sample of galaxies in distant clusters the $e(c)$ spectra are

preferentially found along the fit for normal nearby galaxies (P99). This suggests that dust effects are not relevant in the e(c) spectra of the distant galaxies, while strong extinction alters the emission line properties of all Infrared Luminous galaxies of any spectral class.

Furthermore the median *flux* ratios in W98 are $F([\text{OII}])/F(\text{H}\alpha)=0.23\pm0.18$ (Seyfert1's excluded). These are again a factor of ~ 2 lower than the median flux ratio observed in nearby spirals (0.43 ± 0.27 , K92b).⁴ The difference in *equivalent width* ratio between the W98 sample and normal nearby galaxies is hence entirely due to the difference in the average *flux* ratio of the two lines. This is consistent with the suggestion that the main cause of the low $\text{EW}([\text{OII}])/\text{EW}(\text{H}\alpha + \text{NII})$ is a differential effect of dust extinction on the lines and the underlying continuum.

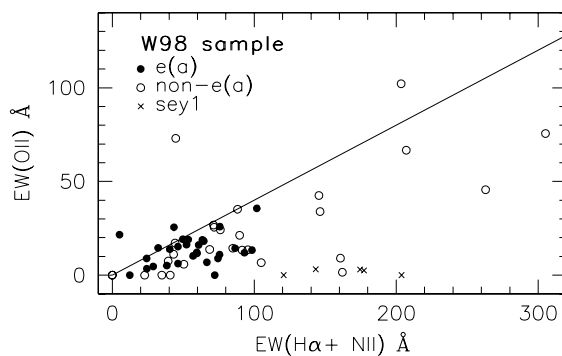


Fig. 3. The line represents the fit for normal field galaxies in the local Universe ($\text{EW}([\text{OII}])=0.4 \text{EW}(\text{H}\alpha + \text{NII})$). See P99, Fig. 5, for a similar plot of the LK95 sample.

We now want to establish whether this hypothesis is in accordance with the values of the color excess $E(\text{B}-\text{V})$ derived by W98b from the Balmer decrement $\text{H}\alpha/\text{H}\beta$. Table 5 lists the median $E(\text{B}-\text{V})$ and the bootstrap standard deviations of the main emission-line classes in the W98 sample.⁵ We note that the e(a) galaxies appear to have a median $E(\text{B}-\text{V})$ significantly higher than the other classes and seem to represent

⁴Note that the value $\text{NII}/\text{H}\alpha$ can be neglected in this discussion because it depends only weakly on $\text{EW}(\text{H}\alpha)$ and it is approximately constant (K92, Tresse et al. 1999).

⁵Seyfert1 spectra have a very low average $E(\text{B}-\text{V})$ (W98b) and have been excluded from this analysis.

TABLE 5
MEDIAN $E(\text{B}-\text{V})$ AS A FUNCTION OF THE SPECTRAL CLASS

Class	Median $E(\text{B}-\text{V})$	SD	N
e(a)	1.11	0.12	34
e(c)	0.68	0.13	18
e(b)	0.62	0.15	5
e	0.80	0.11	36
all	0.86	0.07	93

the most extincted cases in a sample which on average is already very dusty.⁶

In order to verify whether these $E(B-V)$ values can account for the low $[\text{OII}]/\text{H}\alpha$, we first need to determine the *intrinsic* (unreddened) typical ratio. We will assume this to be equal to the *intrinsic* ratio in normal nearby galaxies, which can be derived from the median *observed* ratio in spirals (0.43) correcting for the average extinction (1 mag at $\text{H}\alpha$, K92). The correction in the case of normal spirals therefore corresponds to a factor 2.5 for the $\text{H}\alpha$ flux and a factor about 5 for the $[\text{OII}]$ flux if we assume a foreground screen dust configuration and we adopt the standard Galactic extinction curve for the diffuse medium ($R_V = A_V/E(B-V) = 3.1$, Mathis 1990). Combining the intrinsic typical ratio $[\text{OII}]/\text{H}\alpha_{int}$ (~ 0.85) with the median $E(B-V)$ of our sample (0.86, Table 5), we expect to observe

$$[\text{OII}]/\text{H}\alpha_{exp.} = [\text{OII}]/\text{H}\alpha_{int} * 0.22 = 0.19.$$

This is broadly consistent with the median value observed in W98:

$$[\text{OII}]/\text{H}\alpha_{obs.} = [\text{OII}]/\text{H}\alpha_{int} * 0.27 = 0.23.$$

We stress that there are two arbitrary assumptions in the method used above, namely that the intrinsic line ratio in VLIRGs is equal to the one in normal spirals – when the latter is corrected for the average extinction – and that we can adopt as attenuation curve the extinction curve of the diffuse medium in the Galaxy.⁷ Nevertheless, the high extinction derived from the Balmer decrement ($E(B-V)$) necessarily implies that the emission line ratios must be greatly affected by reddening and the comparison shown above demonstrates that the observed $E(B-V)$ values are *consistent* with the low $[\text{OII}]/\text{H}\alpha$.

3.1. AGN types

On the basis of the standard diagnostic diagrams discussed by Veilleux & Osterbrock (1987), W98b classified the spectra into one of the following types (hereafter “AGN type”): HII galaxy (H), LINER (L), mixture type between HII galaxy and LINER (LH), Seyfert2 (S2), Seyfert1 (S1), unclassified AGN (S?), unclassified because lacking emission lines (O).

The AGN type distribution of each spectral class is shown in Fig. 4. The great majority of e(a)’s are classified as HII galaxies or mixture types between HII galaxy and LINER and only 1 e(a) galaxy has a Seyfert2 spectrum, which is a dubious case between a Seyfert2 and a LINER.⁸ A similar AGN distribution

⁶The $E(B-V)$ differences among the spectral classes could be affected by the uncertainty in the measurement of the underlying line in absorption, however we do not expect any systematic error that could cause an overestimate of the $E(B-V)$ values for e(a)’s: in the spectra with obvious $\text{H}\beta$ absorption, the $\text{H}\beta$ flux in emission has been corrected by W98a performing a multi-component fitting, adopting a Lorentz profile in absorption and one or two Gaussian emission components. If anything, the absorption component is more likely to be unmeasured in the weakest cases (non-e(a) spectra), with a consequent overestimate of $E(B-V)$ resulting in a trend contrary to what is observed.

⁷Adopting as *attenuation curve* any of the *extinction curves* observed in our or nearby galaxies is known to be incorrect in most cases because while the extinction curve depends only on the physical properties of the dust grains, the attenuation curve is determined also by the spatial distribution of stars and gas.

⁸Spectropolarimetric studies indicate that e(a) galaxies do not usually host obscured AGNs, since none of the

is found for the e(c) spectra, while only the e(b) class includes a higher proportion of Seyfert2 galaxies. We conclude that e(a) VLIRGs do not generally display spectral evidence for an AGN and that the only type of “activity” observed in most of these e(a)’s is due to star formation.

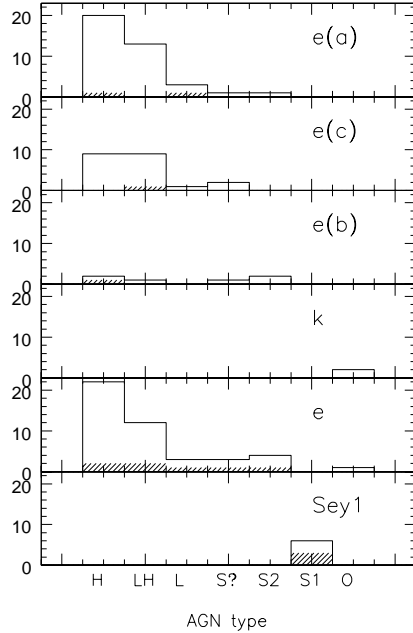


Fig. 4. Histograms showing the distribution of AGN types within each spectral class. The shaded area indicates galaxies with $\log L_{FIR}/L_{\odot} > 12$.

4. The nature of the e(a) galaxies

In this section we compare our spectroscopic results with the FIR and morphological properties with the aim of studying the star formation rates and the merger stage of the e(a) galaxies. An interesting aspect of the comparison of the FIR and $H\alpha$ luminosities is the determination of the amount of star formation that cannot be detected at optical wavelengths, while the analysis of the morphological properties of the e(a)’s can reveal whether they are associated with a specific phase of the merger or with a typical separation between the two merging galaxies.

4.1. Star formation rates

approximately two dozen hidden broad-line regions detected to date are found in objects dominated by a strong Balmer absorption-line spectrum (Tran et al. 1998).

The FIR and $H\alpha$ luminosities are useful indicators of the current star formation rate in dust-enshrouded and dust-free galaxies respectively.

The FIR luminosity distribution of the e(a) galaxies is similar to the one of the whole VLIRG sample (Fig. 5), as shown by a χ^2 test at the 95% confidence level. The median $\log L_{FIR}(L_{\odot})$ is 11.68 for e(a)'s and 11.72 for the whole sample. The slightly higher value found for the e(b)'s (11.87) is significant and is probably due to the fact that the proportion of Seyfert galaxies in this spectral class is higher than in the other classes. Seyfert1's are known to have the highest median FIR luminosity (12.64).

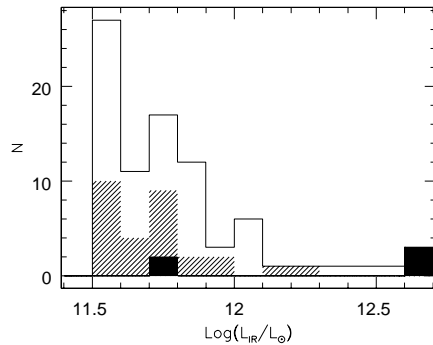


Fig. 5 FIR luminosity distribution of the whole VLIRG sample (empty histogram), of the e(a) subsample (shaded histogram) and of the Seyfert1 subsample (solid histogram).

In Fig. 6 we plot the FIR and $H\alpha$ luminosities of the W98 sample. The $H\alpha$ luminosities have been derived from the fluxes and the distances given in W98a,b. The solid line is the best fit to the datapoints; for comparison we have plotted as a dotted line the relation valid for normal spiral galaxies at low-redshift (Devereux & Young 1990), which typically have $\log L_{FIR}(L_{\odot}) < 10.5$.

The reader should keep in mind that our $H\alpha$ luminosities are derived from *nuclear* spectra while the relation for normal spirals was obtained from large aperture photometry. The fractional contribution of nuclear emission to the total $H\alpha$ luminosities of interacting galaxies is three times higher than the average in isolated spirals (Kennicutt et al. 1987, K87): the median fraction is 13 % and in most cases is smaller/equal to 25 %. Using K87 results and considering that: a) the apertures in W98 are comparable to K87, but the median redshift is higher (0.0324 versus 0.006/0.010); b) in Infrared Luminous mergers the star formation is centrally concentrated and it is reasonable to expect an even higher fractional contribution from the nucleus (Kennicutt 1999, private communication); then a correction factor of 7 in flux can be regarded as an upper limit for the W98 galaxies and it is likely to overestimate the total luminosity. The datapoints for integrated luminosities therefore should lie in Fig. 6 between the solid line (best fit to the data, uncorrected) and the dashed line ($L(H\alpha)*7$).

Even taking the aperture effects into account, the $H\alpha$ luminosities at a given L_{FIR} are much lower in the W98 galaxies than in optically selected spirals, a result which is found in Infrared Luminous samples in

general. Considering only a subset of the data taken during the most favourable weather conditions does not alter this result.

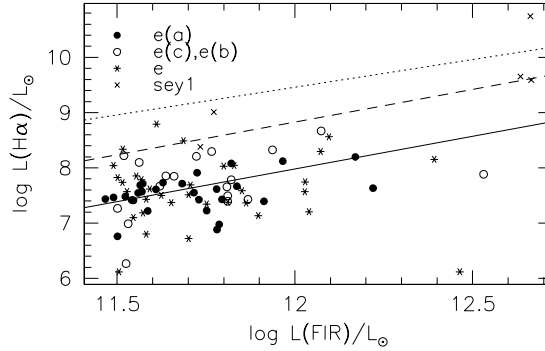


Fig. 6 FIR and H α luminosities in solar units. The best fit to the datapoints is shown as a solid line: $\log L(\text{H}\alpha)(L_{\odot}) = 1.18 \times \log L_{\text{FIR}}(L_{\odot}) - 6.18$. The fit to the e(a) subsample is flatter: $\log L(\text{H}\alpha)(L_{\odot}) = 0.67 \times \log L_{\text{FIR}}(L_{\odot}) - 0.28$. The relation found by Devereux & Young (1990, DY90) for a sample of field spiral galaxies in the local Universe is extrapolated to the FIR luminosities of the present dataset and is shown as a dotted line ($L(\text{H}\alpha)(L_{\odot}) \sim 3 \times 10^{-3} L_{\text{FIR}}(L_{\odot})$), after taking into account the correction for the different spectral FIR range. The dashed line is found from the solid line multiplying $L_{\text{H}\alpha}$ by 7 (see text) and represents the upper limit of the *integrated* luminosity.

This “scarcity” of H α flux is directly mirrored in the SFR estimates, as we will now show. There are many calibrations of the H α luminosity versus the SFR (see Kennicutt 1998 for a review) and they are all found using an evolutionary synthesis model assuming a Case B recombination for ionization bound regions. Here we use the calibration given by Barbaro & Poggianti (1997, BP97)⁹ for a Salpeter IMF in the mass range 0.1–100 M_{\odot} : $\text{SFR}_{\text{H}\alpha} (M_{\odot} \text{ yr}^{-1}) = 1.1 \times 10^{-41} L(\text{H}\alpha) (\text{ergs s}^{-1})$.¹⁰

For estimating the SFR from the FIR luminosity we use the relation given by Kennicutt (1998): $\text{SFR}_{\text{FIR}} (M_{\odot} \text{ yr}^{-1}) = 4.5 \times 10^{-44} L_{\text{FIR}} (\text{ergs s}^{-1})$. This is applicable only if most of the bolometric luminosity is reprocessed in the FIR, as in the case of the sample considered here, and for continuous bursts with ages less than 10^8 years. This latter assumption on the burst duration has not been ascertained for e(a) galaxies, but the adopted SFR calibration lies within $\pm 30\%$ of most of the other published calibrations and has comparable uncertainty. Since both the H α and the FIR calibrations are obtained for the same IMF and are sensitive to the hottest (more massive) young stars, the ratio of the SFRs derived with the two methods is essentially independent from the IMF adopted. Furthermore, the ratio of SFRs is also distance-independent.

⁹The original calibration from BP97 included a factor 0.7 accounting for a fraction of the ionizing photons which is lost due to dust *before* ionizing the gas (see Mayya & Prabhu 1996 for an observational confirmation of this effect). This factor is usually neglected in the other calibrations found in the literature and it has not been included here.

¹⁰With the same IMF and based on an independent synthesis model, Kennicutt (1992b) obtains: $\text{SFR} (M_{\odot} \text{ yr}^{-1}) = 0.89 \times 10^{-41} L(\text{H}\alpha) (\text{ergs s}^{-1})$, and Kennicutt (1998) gives: $\text{SFR} (M_{\odot} \text{ yr}^{-1}) = 0.79 \times 10^{-41} L(\text{H}\alpha) (\text{ergs s}^{-1})$.

The SFRs derived with the two methods are presented in Table 2 and in Fig. 7. The observed relation for e(a)’s is even flatter than for e(c)’s/e(b)’s and corresponds to $SFR_{H\alpha} \sim SFR_{FIR} * C_{ap}/70$, where $1 < C_{ap} < 7$ is the aperture correction to be applied to the $H\alpha$ flux. The errorbars in this relation are dominated by the uncertainties in the conversion between fluxes and SFR, at least 30 % both for the FIR and the $H\alpha$, and in some cases the FIR luminosity is likely to include the emission from both companions.

The median E(B-V) of e(a) galaxies (Table 5) corresponds to an extinction of 2.9 mag at the wavelength of $H\alpha$, if the standard galactic extinction curve for the diffuse interstellar medium is adopted (see §3 for a discussion of the uncertainties connected to this assumption). Neglecting aperture corrections to $H\alpha$, this amount of reddening is not enough to reconcile the $SFR_{H\alpha}$ estimate with the SFR derived from the FIR (dashed line in Fig. 7), while considering both reddening and aperture effects, the two SFR estimates for e(a)’s are in agreement if the upper limit on the aperture correction is used (7). Adopting a more plausible smaller correction, the discrepancy between the two SFRs could indicate that a significant fraction of the FIR emission comes from a galactic region whose line flux is completely extinguished.

From the comparison of FIR and $H\alpha$ estimates of the SFR, we conclude that the SFR derived from the *observed integrated* $H\alpha$ flux in e(a) galaxies is a factor between 10 and 70 lower than the SFR derived from the FIR emission, depending on the appropriate aperture correction to be applied to our sample. Given the low [OII]/ $H\alpha$ ratios of e(a)’s, using the [OII] flux would underestimate the SFR_{FIR} by a further factor of 2, i.e. 20–140 in total.

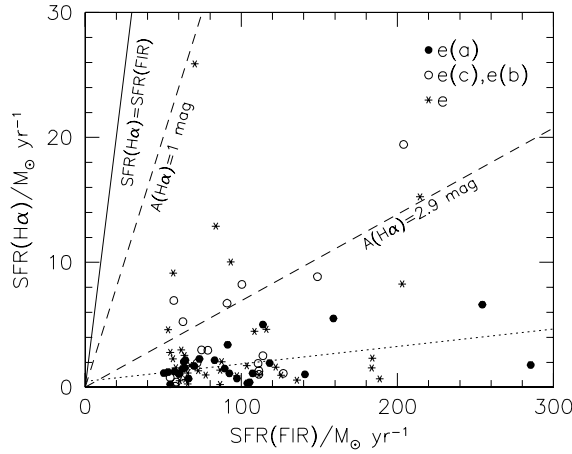


Fig. 7 The SFR derived from the $H\alpha$ line versus the FIR-based estimate (see text for details). *In this plot no aperture correction is applied to the $H\alpha$ flux.* The dotted line is the fit to the e(a) population. The solid line shows the relation $SFR_{H\alpha} = SFR_{FIR}$, and the dashed lines are found for 1 mag extinction at $H\alpha$ (average extinction in K92 nearby spirals) and for the average extinction in e(a)’s in W98 sample as determined by E(B-V) ($A(H\alpha) = 2.9$ mag). The X and Y ranges have been limited for displaying convenience, leaving 7 points out of the diagram.

4.2. Morphological properties

FIR luminous galaxies often show strong interaction or merging signatures (Sanders & Mirabel 1996, Duc et al. 1997); based on optical images from the Digital Sky Survey, W98b assigned a morphological class along a merger sequence (far to near companions 1–4, interacting pairs and mergers 5–6, isolated/advanced mergers 0). The “0” class should include both truly isolated galaxies and objects in an advanced or post merging stage.

In the VLIRG sample the proportion of close mergers is very high for all the spectral classes (Table 6). The ambiguity in interpreting the 0 class complicates the comparison: if the tendency of the e(c)’s to avoid the 5-6 class is real, then maybe a large fraction of the e(c) galaxies of type “0” are truly isolated objects, while the “0” type Seyfert1 are likely to be in an advanced merger stage. The e(a)’s are mostly merging galaxies/interacting pairs or galaxies with close companions. The median *projected* separation between the e(a) galaxies and their companions is 50 kpc and the highest separations observed are 100–150 kpc (W98b).

5. E(a) galaxies in other spectroscopic surveys

In this section we review the detection of e(a) galaxies in other spectroscopy surveys at low and high redshift, in order to identify the common properties shared by all e(a)’s. What follows is not a complete inventory (see P99 for additional references and van Breugel 1999 for radio selected e(a)’s) and we will focus on those observations which can be useful for understanding how the e(a) population evolves with redshift and depends on the environment.

5.1. E(a) galaxies in the local Universe

At low- z , e(a) spectra are present but scarce in optically-selected spectroscopic surveys of field galaxies: P99 noticed that at most 7% (1/14) of the normal non-merging, non-Seyfert galaxies in K92¹¹ show an e(a) spectrum. Hashimoto (1998, private communication) estimated the e(a) frequency to be 8 %

¹¹The e(a) fraction in K92a cannot be considered representative of a complete sample, since this survey is not complete in any sense and consists of nearby galaxies covering a broad range in morphological types, luminosities and star formation properties.

TABLE 6
FRACTION OF VLIRGS OF A GIVEN SPECTRAL CLASS AS A FUNCTION OF MERGING TYPE

Class	0	1–2	3–4	5–6	N
e(a)	0.14±0.07	0.10±0.06	0.21±0.08	0.55±0.14	29
e(c)	0.46±0.19	0	0.15±0.11	0.38±0.17	13
e(b)	0	0	0.20±0.20	0.80±0.40	5
sey1	0.20±0.20	0	0.20±0.20	0.60±0.35	5
e	0.07±0.05	0.13±0.07	0.20±0.08	0.60±0.14	30

in the Las Campanas Redshift Survey (LCRS, see also Fig. 1 in Zabludoff et al. 1996), but the comparison with the W98 sample is uncertain owing to the differences in the classification criteria and in the spectral quality. An analysis of the FIR and morphological properties of the e(a)’s in the LCRS has not yet been undertaken.

As discussed in P99, a high proportion of e(a) spectra is found instead in the LK95 sample: these galaxies were selected for being merging or strongly interacting systems, either in the optical or in the near-infrared, and are all strong FIR emitters. Evidence for a high e(a) incidence is also found in an unusually active compact group of galaxies with strong FIR and CO emission (de Carvalho & Coziol 1999).
¹²

The analysis of the W98 sample of Very Luminous Infrared Galaxies and of the other “e(a)-rich” samples seems to indicate that field/group e(a) galaxies in the local Universe are highly extincted starbursts and that they are preferentially merging/strongly interacting systems. A statistical study of the e(a) occurrence in nearby clusters is not yet available, but we know it must be rare, given the small number of emission-line galaxies present in dense environments at low- z .

5.2. E(a) galaxies at high redshift

The relevance of e(a) spectra for galaxy evolution studies was first discussed by D99/P99 who found that e(a)’s constitute about 10 % of their sample of cluster and field galaxies at $z \sim 0.4 - 0.5$. HST images of e(a) galaxies in these clusters show that at least half of them are involved in a merger or strong interaction (D99, P99). Spectra with e(a) characteristics were previously observed in other spectroscopic surveys of distant clusters (Couch & Sharples 1987, Couch et al. 1994, 1998, Fisher et al. 1998).

At redshifts comparable to the D99 catalog and up to $z = 1$, a population of Balmer strong galaxies with emission is present in the field sample of the Canada-France Redshift Survey (Hammer et al. 1997, H97, see P99 for a discussion). More recently Flores et al. (1998a,b) presented the results of a deep ISO survey of one of the CFRS fields at 6.75 and 15 μ m. At 6.75 μ m 8 out of the 15 detected galaxies have e(a) spectra ($EW(H\delta) \gtrsim 5 \text{ \AA}$ in this case) and lie at $0.07 < z < 0.88$; the remaining ISO sources have Seyfert1/Seyfert2/e(b) spectra. Among other 8 less secure 6.75 μ m sources, 6 display an e(a) spectrum. At 15 μ m most (71 %) of the sources with optical spectroscopy are classified as e(a) galaxies and have a median redshift $\langle z \rangle = 0.76$. The FIR luminosities of the Flores et al. e(a)’s span the range 10.76 to 12.31 $\log L/L_{\odot}$, with a median 11.66 and their moderate $EW(OII)$ are comparable to those in W98 spectra. This is the first confirmation of the IR luminous nature of e(a) galaxies at high redshift, except for the sub-mm detection of a distant e(a) cluster galaxy, #834 in Cl0024+16 (Smail et al. 1998a). Preliminary results of other field ISO surveys seem to reinforce this conclusion (Elbaz et al. 1999); in distant clusters, Duc et al. (1999) detect at 15 μ m all the e(a) galaxies in the cluster A1689 ($z \sim 0.2$) and confirm their dusty nature and high star formation rates.

The e(a) phenomenon is obviously widespread both at low and high redshifts and involves a high fraction of galaxies in all the FIR luminous samples at any z studied so far. In the distant Universe e(a)’s

¹²At least 14 % of our VLIRGs are in groups or multiple-merging systems. An evolutionary connection between ULIRGs/VLIRGs and compact groups has been suggested by W98b.

are numerous both in the field and in the cluster environment; a systematic census at low- z will be needed to assess the amount of evolution of the e(a) population and its dependence on the environment.

6. Discussion

We have seen in §3 that e(a) spectra are exceptionally numerous among VLIRGs, but their incidence in the W98 sample (Table 4) is based on nuclear spectra, while distant galaxy spectra should be more appropriately compared with *integrated spectra* of low-redshift galaxies. We can evaluate the relevance of aperture effects from the catalog of LK95 which gives both nuclear and whole aperture/integrated spectra of the merging galaxies: in 3 out of the 16 e(a)’s the galaxy has an e(a) nuclear spectrum and a different whole aperture/integrated spectral type, suggesting that a spectroscopic survey of distant galaxies could miss about 20 % of the “nuclear” e(a) population.

In §3 we also noted that no k+a’s are found in our sample. This suggests that the k+a/a+k galaxies are not very luminous FIR emitters and this result is consistent with the lack of emission lines in their optical spectrum and with the *post*-starburst interpretation. Zabludoff et al. (1996) found that at least 5 of the 21 low-redshift “E+A’s” (= k+a/a+k according to our definition) galaxies in the Las Campanas Redshift Survey have clear tidal features. The absence of this type of spectra in the W98 sample implies that if a merger/strong interaction is the mechanism responsible for the field k+a/a+k galaxies at low redshift, they are probably observed during an evolved (post) merger stage, as Zabludoff et al. suggest.

We would like to stress here that *by definition* k+a (“E+A”) spectra have *no detectable emission lines* (Dressler & Gunn 1983), at least at the level of the [OII] detection limit of the available spectroscopic surveys of distant galaxies (typically 3 Å). Unfortunately in the literature this notation has sometimes been used for emission-line galaxies. This work demonstrates once more that the presence/lack of emission lines is not merely a “spectral detail”, but reveals a current/absent star formation activity and discriminates between post-starburst and dusty starburst galaxies. The possibility of an evolutionary connection between k+a’s and e(a)’s has been discussed in P99, who also noted that some of the k+a spectra might be extreme cases of e(a) galaxies, in which the [OII] line is totally obscured by dust.

6.1. The physical origin of the e(a) spectra

In the following we want to investigate the physical origin of the e(a) spectral characteristics, namely a) the strong H δ line in absorption and b) the low [OII]/H α ratio.

On the basis of dust-free models (P99), e(a) spectra can be interpreted as *post-starburst* galaxies with some residual star formation¹³, but the analysis of W98 and other samples (§5) shows that whenever

¹³A similar interpretation is proposed by Flores et al. 1998b, who found their ISO data to be consistent with the scenario of strong starburst episodes followed by the last phases of the burst, where the IR emission is still high due to dust heating by intermediate-mass stars (1–3 M_{\odot}).

the discriminating data (IR) are available, e(a) galaxies are found to be starbursts which contain a large amount of dust, hence we cannot safely rely on dust-free models to estimate their SFRs and histories.

As discussed in §4.1, the low $[\text{OII}]/\text{H}\alpha$ ratios are probably due to the high dust extinction which affects the emission line fluxes – generated inside the HII regions – much more than the stellar underlying continuum coming from populations that are more widely distributed throughout the galaxy (Calzetti et al. 1994, Mayya & Prabhu 1996). In principle other factors influence $[\text{OII}]/\text{H}\alpha$, such as metallicity,¹⁴ or high ionization,¹⁵ but we have shown that the most probable cause of the observed ratios is the high extinction which is implied by the $E(B-V)$ values derived from the Balmer decrement.

A selective extinction is also capable of explaining the strong $\text{H}\delta$ line in absorption, which mostly arises from stars with lower mass/effective temperature (7000-14000 K) than the O, B stars that ionize the gas (> 25000 K). The stellar generations responsible for the strong $\text{H}\delta$ line, with ages between a few 10^7 and $1.5 \cdot 10^9$ yrs (Poggianti & Barbaro 1996, 1997), have had the time to drift away from (or disperse) the dusty molecular clouds where they were born (Calzetti et al., 1994 and references therein) and their emission dominates the integrated spectrum at $\lambda \sim 4000 \text{ \AA}$ if younger stars (causing the emission filling and with lower stellar $\text{EW}(\text{H}\delta)$) are more heavily obscured. Observing an $\text{EW}(\text{H}\delta) > 4 \text{ \AA}$ therefore suggests that the on-going starburst started at least $4 - 5 \cdot 10^7$ yrs before the time of the observation.

A simple way to depict this scenario is to imagine that *the extinction towards a star/stellar population decreases with the stellar age* (Kinney, private communication): the effect of dust is maximum for the youngest generation of stars (that provide the ionizing flux responsible for the emission lines, timescale $< \text{few times } 10^7 \text{ yr}$), and decreases for older stars. In a sense, this scenario is equivalent to a “clumpy distribution of dust” where the location and thickness of the patches are not random, but depend on the age of the embedded stellar populations. The integrated emerging spectrum at wavelength λ is hence dominated by the less extincted (older) stars that are strong emitters at that λ , or that are indirectly responsible for the flux F_λ (for example for the nebular emission).¹⁶ This happens because only the least obscured regions give the major contribution to the integrated spectrum (Witt et al. 1992).

An age-dependent obscuration is expected to mark in a peculiar way the spectrum of a dust-enshrouded starburst. If dust is absent, each given portion of a galactic spectrum is due to the stellar populations of a specific range of ages: for example, the emission lines are only observed if young stars with age $< 4 \cdot 10^7$ yrs are present, while in a star-forming galaxy the U band light is influenced by stars of ages $< 10^9$ yrs. Considering now the effects of dust, if each stellar age corresponds to a different amount of obscuration, *within the same spectrum* we expect to measure different values of extinction, depending on the spectral region/feature used to estimate it. For example, UV-based reddening measurements should underestimate the extinction of the emission lines.

¹⁴The line ratio is expected to decrease with increasing metallicity for an HII region with Z higher than solar (Stasinska 1990), but an analysis of the R_{23} indices (Zaritsky et al. 1994) of W98 galaxies rules out exceptionally high abundances.

¹⁵High ionization is ruled out from the observed $[\text{OIII}]/\text{H}\beta$ (W98b).

¹⁶The FIR flux can be influenced by stars in a quite broad age range, but in starbursts it is mostly affected by the youngest populations and the fact that a fraction of the stars in starbursts seem to be embedded in optically thick dust clouds (Calzetti et al. 1995) suggests that a non-negligible fraction of the FIR emission arises from the innermost layer of the dusty “onions”.

Observational evidence supports this scenario; the extinction values derived by techniques using different spectral ranges/features generally disagree (Fanelli et al. 1988, Bohlin et al. 1990, Keel 1993, Calzetti et al. 1994, Veilleux et al. (1995), Lancon et al. 1996, Mayya & Prabhu 1996, Calzetti 1997,1998, Mas-Hesse & Kunth 1999): the reddening of the UV/optical stellar continuum in starburst galaxy spectra is lower than the reddening of the ionized gas, and this latter is lower than the one inferred from the comparison of the Balmer fluxes with the nebular free-free radio emission (Israel & Kennicutt 1980, Viallefond et al. 1982, Caplan & Deharveng 1986).

Mid/Far-IR and optical studies with good spatial resolution (see e.g. Hwang et al. 1999) hopefully will provide a means to investigate the spatial segregation of the various spectral components and the selective nature of dust extinction in the integrated spectra of starburst galaxies.

7. Summary

- The analysis of a complete sample of Very Luminous InfraRed Galaxies confirms that emission-line spectra with a strong H δ line in absorption (e(a) spectra) are numerous among FIR luminous galaxies, as suggested by P99. More than 50 % of the VLIR galaxies show such a spectrum, in contrast with optically selected galaxy samples where the e(a) fraction is small, but an accurate assessment of this small e(a) fraction awaits a similar spectral analysis on a well-defined control sample of non-IRAS galaxies. The incidence of e(a) galaxies in the different samples seems to suggest that the e(a) signature is capable of identifying from optical data alone a population of heavily extincted starburst galaxies, while neither the moderate strength of their emission lines nor their optical colors (P99, Trentham et al. 1999, Elbaz et al. 1999) can distinguish them from galaxies with more modest rates of star formation. We note that these results do not rule out a viable alternative producing e(a) spectra, although no such case is known yet: a post-starburst galaxy with some residual star formation (P99). A systematic study of optically-selected e(a) galaxies is required to establish the occurrence of this type of e(a)'s.

- The median FIR luminosity of e(a) galaxies in our sample is $\log L_{FIR}/L_{\odot} \leq 11.68$, but we stress that this should be regarded as an upper limit to the whole FIR luminosity distribution of e(a)'s which needs to be determined from the analysis of spectroscopic catalogs including galaxies with $\log L_{FIR}/L_{\odot} < 11.5$ (Kim et al. 1995). While UltraLuminous InfraRed Galaxies can be found efficiently up to very high redshifts by SCUBA at sub-mm wavelengths, the e(a) signature may help to identify less extreme, but more common dust-enshrouded galaxies and it appears to be essentially free from AGN contamination.

- A universal property of the e(a) spectra appears to be a low [OII]/H α equivalent width ratio; we find this to be due to a correspondingly low flux ratio, which is equal to 1/2 of the value observed in nearby spirals. We interpret this result as an effect of dust extinction, which is consistent with the average color excess E(B-V) derived from the Balmer decrement. We propose a scenario of *selective* dust obscuration that affects the youngest stellar populations more than the older stars and that can explain also the strong H δ absorption lines observed.

- The star formation rates derived from the FIR luminosities of the e(a) galaxies lie in the range 50-300 $M_{\odot} yr^{-1}$; SFR estimates based on the H α (and [OII]) luminosities yields values a factor of 10-70 (20-140) lower.

- The incidence of mergers/strong interactions is very high in Very Luminous Infrared Galaxies of any

spectral class and the only notable difference among the classes is a higher proportion of e(c) galaxies with no obvious sign of interaction with a companion, which could be either advanced mergers or truly isolated objects. About 75% of our e(a) galaxies are mergers/interacting pairs with close companions.

- A significant population of e(a) galaxies has been found by deep optical spectroscopic surveys both in the cluster and the field environment at $z \sim 0.4 - 0.5$ (D99, P99, H97). In the low- z Universe, a systematic census of e(a)’s is needed in order to assess the amount of evolution as a function of redshift and environment.

Acknowledgements

We wish to thank C. Liu and R. Kennicutt for providing us their spectrophotometric atlas of merging galaxies and we acknowledge the availability of the Kennicutt’s (1992a) atlas of galaxies from the NDSS-DCA Astronomical Data Center. This work has greatly benefited from discussions with Ian Smail, Pierre-Alain Duc, Steve Maddox, Robert Kennicutt, Paola Mazzei, Guido Barbaro and Fabio Governato, and has been supported in part by the Formation and Evolution of Galaxies network set up by the European Commission under contract ERB FMRX-CT96-086 of its TMR program. HW acknowledges support from the Royal Society China Royal Fellowship scheme.

REFERENCES

- Altieri, B., Metcalfe, L., Kneib, J. P., McBreen, B., Aussel, H., Biviano, A., Delaney, M., Elbaz, D., Leech, K., Lemonon, L., Okumura, K., Pello, R., Schulz, B., 1999, A&A in press (astro-ph 9810480)
- Aussel, H., Cesarsky, C. J., Elbaz, D., Starck, J. L., 1999, A&A, 342, 313
- Barbaro G. & Poggianti B. M., 1997, A&A, 490, 504
- Barger, A., Cowie, L., Sanders, D., Fulton, E., Taniguchi, Y., Sato, Y., Kaware, K., Okuda, H., 1998, Nature, 394, 248
- Bohlin, R. C., Cornett, R. H., Hill, J. K., Stecher, T. P., 1990, ApJ, 363, 154
- Calzetti, D., Kinney, A. L., Storchi-Bergmann, T., 1994, ApJ, 429, 582
- Calzetti, D., Bohlin, R. C., Kinney, A. L., Storchi-Bergmann, T., Heckman, T. M., 1995, ApJ, 443, 136
- Calzetti, D., 1997, AnJ, 113, 162
- Calzetti, D., 1998, in *Dwarf Galaxies and Cosmology*, eds. Thuan et al., in press
- Caplan, J., Deharveng, L., 1986, A&A, 155, 297
- Cimatti, A., Andreani, P., Rottgering, H., Tilanus, R., 1998, Nature, 392, 895
- Clements, D. L., Desert, F.-X., Franceschini, A., Reach, W. T., Baker, A. C., Davies, J. K., Cesarsky, C., 1999, A&A in press (astro-ph 9901267)
- Cohen, J. G., Hogg, D. W., Blandford, R., Pahre, M. A., Shopbell, P. L., in *Infrared Surveys: A Prelude to SIRTf*, in press (astro-ph 9808343)
- Couch W. J., Sharples R. M., 1987, MNRAS, 229, 423 (CS87)
- Couch, W. J., Ellis, R. S., Sharples, R. M., Smail, I., 1994, ApJ, 430, 121

- Couch W. J., Barger A. J., Smail, I., Ellis R. S., Sharples R. M., 1998, *ApJ*, 497, 188
- de Carvalho, R. R., & Coziol R., 1999, preprint (astro-ph 9901006)
- Devereux, N. A., Young, J. S., 1990, *ApJ*, 350, L25
- Dey, A., Graham, J. R., Ivison, R. J., Smail, I., Wright, G. S., Liu, M., 1999, *ApJ*, submitted (astro-ph 9902044)
- Dickinson, M., 1998, in *Hubble Deep Field*, eds. Livio et al., p. 219
- Dressler A., Gunn J. E., 1983, *ApJ*, 270, 7
- Dressler, A., Smail, I., Poggianti, B. M., Butcher, H., Couch, W. J., Ellis, R. S., Oemler, A. Jr., 1999, *ApJS*, in press (D99) (astro-ph 9901263)
- Duc, P. A., Mirabel, I. F., Maza, J., 1997, *A&AS*, 124, 533
- Duc, P. A., Poggianti, B. M. et al, 1999, in preparation
- Elbaz, D., Aussel, H., Cesarsky, C. J., Desert, F. X., Fadda, D., Franceschini, A., Puget, J. L., Starck, J. L., 1998, in *Next Generation Space Telescope*, Proc. of 34th Liege Intern. Astroph. Colloquium, in press
- Elbaz, D., Aussel, H., Cesarsky, C. J., Desert, F. X., Fadda, D., Franceschini, A., Harwit, M., Puget, J. L., Starck, J. L., 1999, in *The Universe as Seen by ISO*, eds. Cox & Kessler, in press (astro-ph 9902229)
- Ellis, R. S., 1998a, *ARAA*, 35, 389
- Ellis, R. S., 1998b, *Nature*, 395, A3 (reviews)
- Fanelli, M. N., O’Connell, R. W., Thuan, T. X., 1988, *ApJ*, 334, 665
- Fisher, D., Fabricant, D., Franx, M., van Dokkum, P., 1998, *ApJ*, 498, 195
- Flores, H., Hammer, F., Desert, F. X., Cesarsky, C., Thuan, T. X., Crampton, D., Eales, S., Le Fevre, O., Lilly, S. J., Elbaz, D., Omont, A., 1998a, *A&A* in press (astro-ph 9811201)
- Flores, H., Hammer, F., Thuan, T. X., Cesarsky, C., Desert, F. X., Omont, A., Lilly, S. J., Eales, S., Crampton, D., Le Fevre, O., 1998b, *ApJ* in press (astro-ph 9811202)
- Glazebrook, K., Blake, C., Economou, F., Lilly, S., Colless, M., 1999, *MNRAS* in press (astro-ph 9808276)
- Graham, J. R., Dey, A., 1996, *ApJ*, 471, 720
- Hammer, F., Flores, H., Lilly, S. J., Crampton, D., Le Fevre, O., Rola, C., Mallen-Ornelas, G., Schade, D., Tresse, L., 1997, *ApJ*, 481, 49 (H97)
- Helou, G., Khan, I. R., Malek, L., Boehmer, L., 1988, *ApJS*, 68, 151
- Hughes, D., Serjeant, S., Dunlop, J., et al., 1998, *Nature*, 394, 241
- Hwang, C-Y., Lo, K. Y., Gao, Y., Gruendl, R. A., Lu, N., 1999, *ApJL*, 511, L17
- Israel, F. P., Kennicutt, R. C., 1980, *Astrophys. Letters*, 21, 1
- Keel, W. C., 1993, in *Massive Stars: Their Lives in the Interstellar Medium*, ASP Conf. Ser. vol. 35, p.498
- Kennicutt, R. C. Jr, 1992a, *ApJS*, 79, 255
- Kennicutt, R. C. Jr, 1992b, *ApJ*, 388, 310
- Kennicutt, R. C. Jr, Keel, W. C., van der Hulst, J. M., Hummel, E., Roettiger, K. A., 1987, *AnJ*, 93, 1011
- Kennicutt, R. C. Jr, 1998, *ARAA*, 36, 189
- Kim, D. C., Sanders, D. B., Veilleux, S., Mazzarella, J. M., Soifer, B. T., 1995, *ApJS*, 98, 129
- Lancon, A., Rocca-Volmerange, B., Thuan, T. X., 1996, *A&AS*, 115, 253

- Lilly, S. J., Eales, S. A., Gear, W. K. P., Hammer, F., Le Fevre, O., Crampton, D., Bond, J. R., Dunne, L., 1999, ApJ in press (astro-ph 9901047)
- Liu, C.T., Kennicutt, R. C. Jr, 1995a, ApJS, 100, 325
- Liu, C.T., Kennicutt, R. C. Jr, 1995b, ApJ, 450, 547
- Mas-Hesse, J. M., Kunth, D., 1999, A&A in press (astro-ph 9812072)
- Mathis, J. S., 1990, ARAA, 28, 37
- Mayya, Y. D., Prabhu, T. P., 1996, AnJ, 111, 1252
- Metcalf, L., Altieri, B., McBreen, B., Kneib, J-P., Delaney, M., Biviano, A., Kessler, M. F., Leech, K., Okumura, K., Schulz, B., Elbaz, D., Aussel, H., 1999, in *The Universe as seen by ISO*, eds. Cox & Kessler, in press, (astro-ph 9901147)
- Meurer, G., Heckman, T. M., Lehnert, M. D., Leitherer, C., Lowenthal, J., 1997, AnJ, 114, 54
- Oliver, S., Rowan-Robinson, M., Cesarsky, C., et al., 1999, in *Wide-field Surveys in Cosmology*, Proc., XIV IAP Meeting, in press (astro-ph 9901274)
- Pettini, M., Kellogg, M., Steidel, C. C., Dickinson, M., Adelberger, K. L., Giavalisco, M., 1998, ApJ, 508, 539
- Poggianti B. M. & Barbaro G., 1996, A&A, 314, 379
- Poggianti B. M. & Barbaro G., 1997, A&A, 325, 1025
- Poggianti, B. M., Smail, I., Dressler, A., Couch, W. J., Barger, A. J., Butcher, H., Ellis, R. S., Oemler, A., 1999, ApJ, in press (P99) (astro-ph 9901264)
- Puget, J. L., et al., 1999, A&A in press (astro-ph 9812039)
- Sanders, D. B., Mirabel, I. F., 1996, ARAA, 34, 749
- Smail, I., Ivison, R., Blain, A., 1997, ApJ, 490, L5
- Smail, I., Ivison, R., Blain, A., Kneib, J-P, 1998a, ApJ, 507, L21
- Smail, I., Ivison, R., Blain, A., Kneib, J.-P., 1998b, in *After the Dark Ages: When Galaxies Were Young (the Universe at $2 < z < 5$)*, in press (astro-ph 9810281)
- Spinrad, H., Dey, A., Stern, D., Dunlop, J., Peacock, J., Jimenez, R., Windhorst, R., 1997, ApJ, 484, 581
- Stasinska, G., 1990, A&AS, 83, 501
- Steidel, C. C., Adelberger, K. L., Dickinson, M., Giavalisco M., Pettini, M., 1998, in *The Birth of Galaxies*, in press (astro-ph 9812167)
- Steidel, C. C., Adelberger, K. L., Giavalisco, M., Dickinson, M., Pettini, M., 1999, ApJ in press (astro-ph 9811399)
- Strauss, M. A. et al., 1992, ApJS, 83, 29
- Tran, H. D., Brotherton, M. S., Stanford, S. A., van Breugel, W., Dey, A., Stern, D., Antonucci, R., 1998, ApJ in press (astro-ph 9812110)
- Trentham, N., Kormendy, Sanders, D. B., 1999, AnJ, in press (astro-ph 9901382)
- Tresse, L., Maddox, S., Loveday, J., 1999, MNRAS, submitted
- Treu, T., Stiavelli, M., Walker, A. R., et al., 1999, A&A, in press (astro-ph 9808282)
- van Breugel, W., 1999, in *Ultraluminous Galaxies: Monsters and Babies*, in press (astro-ph 9902048)
- Veilleux, S., Osterbrock, E., 1987, ApJS, 63, 295
- Veilleux, S., Kim, D. C., Sanders, D. B., Mazzarella, J. M., Soifer, B. T., 1995, ApJS, 98, 171

- Viallefond, F., Goss, W. M., Allen, R. J., 1982, A&A, 115, 373
- Witt, A. N., Thronson, H. A., Capuano, J. M., 1992, ApJ, 393, 611
- Wu, H., Zou, Z. L., Xia, X. Y., Deng, Z. G., 1998a, A&AS, 127, 521 (W98a)
- Wu, H., Zou, Z. L., Xia, X. Y., Deng, Z. G., 1998b, A&AS, 132, 181 (W98b)
- Zabludoff A. I., Zaritsky D., Lin H., Tucker D., Hashimoto Y., Shectman S.A., Oemler A., Kirshner R. P., 1996, ApJ, 466, 104
- Zaritsky D., Kennicutt R. C. Jr., Huchra J. P., 1994, ApJ, 420, 87